Study on regeneration performance of carbon fluoride adsorbent in SF_6 gas

Wei CHENG [a*], Feng ZHU [b], Chen HANG [c], ZhengJie XU [d]

State Grid Anhui Electric Power Co., Ltd. Electric Power Science Research Institute, Hefei, Anhui, China

Abstract: To study the regeneration of CF-100 type microcrystalline material after adsorbing carbon fluorides in SF_6, an experimental device was built that can achieve both vacuum desorption of carbon fluorides and auxiliary heating to promote vacuum desorption of carbon fluorides. Thermogravimetric analyzer and Fourier transform infrared spectrometer were used to analyze the optimal treatment temperature and time of regeneration technology for promoting vacuum desorption of fluorocarbon by auxiliary heating. A comparative study was conducted on the two regeneration techniques mentioned above by analyzing the relationship between adsorption performance and the number of regenerations. The regeneration effects were also validated by using a specific surface area tester to examine the test data. The results demonstrate that desorption of fluorocarbons from CF-100 microcrystalline material is more efficient using a vacuum desorption method aided by auxiliary heating, as opposed to pure vacuum desorption. The CF-100 type of microcrystalline material achieves the best desorption effect when heated to 300℃ with an auxiliary heating duration of 2 h, with an activation energy of 293.933 KJ/mol. After activation, CF-100 microcrystalline materials exhibit stable adsorption and desorption performance for decarbonization and possess excellent recyclability.

1 Introduction

Sulfur hexafluoride (SF_6) is extensively employed in high-voltage electrical apparatus owing to its exceptional insulating and arc-extinguishing characteristics, alongside its chemical stability[1, 2]. The operation and maintenance experience shows that electrical equipment utilizing SF_6 gas generates a noteworthy quantity of carbon fluorides (e.g. C_2F_6 and C_3F_8) during extended periods of functioning. This results in a diminished capacity for both insulation and arc extinguishing properties of SF_6 gas. Therefore, in order to ensure the safe and stable operation of electrical equipment, it is necessary to replace the SF_6 gas in the gas chamber when the impurity gas content is high as mentioned above. However, SF_6 gas, as one of the six greenhouse gases explicitly required to be restricted in Kyoto Protocol, is obviously not in line with the target of "double carbon" if it is directly discharged after being replaced. To achieve green development, current grid enterprises will purify the retired SF_6 gas to meet the new gas standards in GB/T 12022 Industrial Hexafluoride, which requires C_2F_6 content in SF_6 gas to be ≤200 ppmw and C_3F_8 content to be ≤50 ppmw, in order to accomplish SF_6 gas recycling[3,4]. Currently, deep cryogenic distillation is mainly used to remove fluorocarbons from SF_6 gas. However, this method has a slow purification rate and high energy consumption, which is not in line with the concept of low carbon[5]. In comparison, the utilization of adsorbent adsorption presents numerous benefits including prompt purification velocity, reduced energy consumption, convenience in operation and regeneration, which largely render it an optimal purification means. Nonetheless, in the present, there exists a limited number of investigations pertaining to adsorbents amenable to adsorbing carbon fluoride in SF_6 gas, and these have yet to be employed in practical engineering applications. The CF-100 microcrystalline material adsorbent was examined and evaluated by the author, and the outcomes of the static adsorption test are presented in Table 1. This particular adsorbent displays remarkable aptitude in averting the co-adsorption occurrence during the separation process of SF_6 gas from fluorocarbon, while exhibiting commendable performance in terms of adsorption and separation[6-8]. The adsorbent will reach its saturation point upon adsorbing a considerable amount of impurity gas, necessitating the replacement or regeneration of the adsorbent to uphold its capacity for adsorption and separation efficacy. Nevertheless, the exorbitant cost of microcrystalline materials proves to be a significant impediment to their direct substitution with new adsorbents. Furthermore, the typical placement of adsorbents within the adsorption tower in the purification equipment necessitates the need for frequent disassembly, which not only entails intricate operations but also exacerbates the risk of gas leakage. The rejuvenation of the adsorbent primarily employs technological methods

[a*]Corresponding author: ali88945@sina.com, [b] feng342524@126.com, [c] whhangchen@126.com, [d] XuZhengJie129@163.com

such as nitrogen replacement, heating, and vacuuming[9]. This process enables the adsorbent to transition from a state of adsorption saturation to a non-adsorption state, or a state of minimal adsorption, without necessitating the replacement of the adsorbent. This method is characterized by its simplicity of operation and its marked efficacy in addressing the problem of adsorbent saturatio.

Table 1 Experimental data of CF-100 microcrystalline material adsorbing fluorocarbon in SF_6.

Adsorbent dosage /kg	Adsorption pressure /Mpa	Adsorption state	C_2F_6 /ppm	C_3F_8 /ppm
2	0.4	Before	550.81	88.60
		After	425.32	55.99

Currently, the predominant application of the purification and recovery device is to achieve the adsorption and segregation of carbon fluoride in SF_6 gas. However, nitrogen purging necessitates an external gas source, consequently augmenting the burden of manual upkeep and failing to meet the genuine engineering prerequisites. Therefore, this paper studies the regeneration technology of fluorocarbon adsorbent in SF_6 gas based on vacuum regeneration and vacuum desorption regeneration of auxiliary heating: An experimental device that can realize vacuum regeneration and high temperature regeneration at the same time was built, and the desorption regeneration of fluorocarbon adsorbent was studied, and the optimal desorption regeneration mode was selected by studying the relationship between adsorption performance and regeneration times of adsorbent. By conducting an analysis of the TG/DTG thermogravimetric curve and Fourier infrared spectrum structure, the optimal desorption temperature and duration were determined. Compare the specific surface area and pore size of the adsorbent before and after regeneration to evaluate the desorption performance, so as to achieve efficient regeneration of microcrystalline material adsorbent and realize the removal of carbon fluoride in SF_6.

2 Experiment

2.1 Sample Treatment and Characterization Experiment

2.1.1 Sample Pretreatment of Microcrystalline Materials

The specimens employed in the investigation were microcrystalline materials denoted as CF-100, which were acquired from Hubei Shentan Environmental Protection New Materials Co., Ltd. The microcrystalline materials without adsorption, after adsorption saturation and after regeneration experiment are respectively marked as three groups: A, B and C. Each group of adsorbents is divided into several parts, each part is 10 g.

The main experimental and analytical instruments used are shown in Table 2:

Table 2 Main experimental and analytical instruments

Instrument name	Model	Manufacturer
FESEM	Hitachi SU8010	Hitachi, Japan
Thermogravimetric analyzer(TG)	TGA/DSC3+	Mettler Toledo, Switzerland
Fourier transform infrared spectrometer(FTIR)	Nicolet IS10	Thermo Fisher Scientific
Full-automatic specific surface area and void analyzer	ASAP 2460	Micromeritics

2.1.2 Experimental steps of adsorbent characterization

(1) SEM experiment

A conventional cold field emission scanning electron microscope (SEM, Hitachi SU8010, Hitachi, Japan) was employed to analyze the micro-morphology of group A microcrystalline materials without adsorption and group B microcrystalline materials with adsorption. The conductive tape was affixed onto the sample stage, and subsequently, a small portion of microcrystalline material from groups A and B was placed onto the surface of the conductive double-sided tape separately. Lastly, the samples were observed following gold spraying using a gold spraying instrument.

(2) TG experiment

Temperature is the most direct factor affecting the desorption effect of adsorbent. Thermogravimetric analyzer (TGA/DSC3+, Mettler Toledo, Switzerland) was used to analyze the pyrolysis characteristics of group B microcrystalline materials at different heating rates (5, 10, 20 and 30 ℃/min), and it was found that the desorption effect changed significantly at different temperatures, so as to obtain the best desorption temperature of group B microcrystalline materials. Due to the discernible impact of numerous factors on the thermogravimetric experiment, it is imperative to devise an experimental arrangement that can eliminate extraneous variables and guarantee the validity of the results afore conducting the experiment. Hence, prior to embarking upon the experimental procedures, it is imperative to perform calibration of the balance, desiccate the samples, and guarantee that the sample size is within the range of 1/3 to 1/2 of the crucible volume for the execution of repeated experiments. Take about 10 mg of the sample and put it in a ceramic crucible with holes. The carrier gas flow is high-purity nitrogen (N_2), the flow rate is set to 50 mL/min, and the final temperature of the experiment is set to 900℃. After the thermogravimetric experiment, the thermogravimetric (TG) and differential thermogravimetric (DTG) curves of group B microcrystalline materials are obtained respectively.

(3) FTIR experiment

The optimal desorption time of microcrystalline materials in groups A and B was analyzed using a Fourier transform infrared spectrometer produced by Thermo Fisher Scientific. Samples from group A and group B, with a particle size below 2 μm and mass ranging from 1-2 mg, were co-ground together with 200 mg of potassium bromide (KBr). After uniformly mixing the adsorbent and

KBr, the resulting mixture was then shaped into transparent sheets through the use of an oil press for subsequent determination. Set the wave number range of infrared scanning: 4000~400 cm^{-1}; The temperature of the infrared gas delivery pipe and the gas detection cell is set to 250℃; The scanning frequency is: 8 times/min; Resolution of scanning: 0.4 cm^{-1}.

2.2 Experimental study on regeneration performance of adsorbent

2.2.1 Composition and process of experimental device

(1) Composition of experimental device

This experiment designed and built a Carbfluoride adsorbent desorption experimental device as shown in figure 1, which can simultaneously achieve the functions of vacuum desorption with auxiliary heating and vacuum desorption. It mainly consists of an adsorption column, heating system, vacuum pumping system, analysis system, tail gas treatment system, and data processing system. The adsorption column is an experimental container for microcrystalline materials to adsorb carbon fluoride. The gas outlet end of the adsorption column is equipped with a needle valve and a quick-release connector, which is easy to disassemble; The heating system consists of a heating and thermal insulation steel sleeve wrapped on the surface of the adsorption column, which plays the role of thermal insulation and temperature control; The vacuum pump in that vacuumize system is used for vacuum regeneration to vacuumize the device to remove impurity gas; The gas concentration detector in the analysis system is used to detect the desorbed fluorocarbon gas in the adsorption column pumped by the vacuum pump; The tail gas treatment system is used to treat the desorbed tail gas containing C_2F_6, C_3F_8, etc. In the data processing system, the computer is used to collect and sort out the data of pressure, temperature and gas detection system.

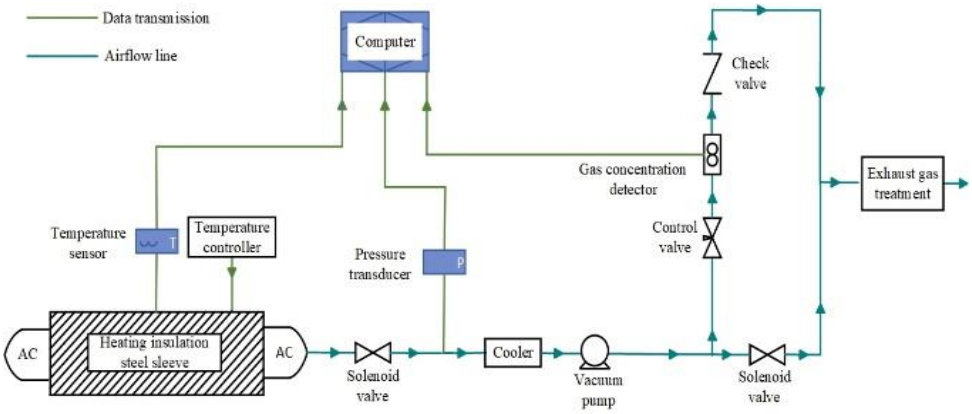

Fig. 1 Experimental device for desorption of fluorocarbon adsorbent

(2) Experimental process

In the vacuum desorption regeneration experiment, the adsorption column is pumped to vacuum by a vacuum pump, and the adsorbent is desorbed and regenerated in a vacuum environment. The specific operation flow is as follows: ① After the adsorption saturation experiment, the adsorption column filled with microcrystalline material is installed on the desorption experimental device; ② Turn on the vacuum pump to vacuum the adsorption column to 133 Pa for 60 min; ③ Close the vacuum pump and the outlet valve at the back end of the adsorption column, and the vacuum regeneration is finished.

In the vacuum desorption regeneration experiment employing auxiliary heating, the microcrystalline material undergoes rejuvenation utilizing the method of vacuum desorption with auxiliary heating. Initially, the heat preservation steel casing is subjected to high temperature in accordance with the predetermined temperature (established through thermogravimetric analysis) to activate the carbon fluorides adsorbent existing within the adsorption column. Following this, a vacuum pump is utilized to conduct evacuation of the adsorption column.

During the above-mentioned desorption experiment, the volume fraction changes of C_2F_6 and C_3F_8 in the desorption gas were monitored in real time to judge the desorption degree of C_2F_6 and C_3F_8 on the adsorbent. When the gas concentration is detected that the volume fraction of C_2F_6 and C_3F_8 becomes 0, the regeneration is terminated, and both the detected tail gas and the desorbed gas pass through the tail gas treatment device, so as to solve the problems of safety hazards and emission pollution caused by carbon-containing fluoride gas.

3 Results and discussion

3.1 Micro-morphological analysis

In order to explore the difference of micro-morphology of CF-100 microcrystalline materials before and after adsorption of fluorocarbon in SF_6 gas, it was characterized by SEM. As shown in Figure 2, scanning images with scanning widths of 1 μm, 10 μm and 50 μm and working voltage of 3.0 kV were selected during the experiment. As can be seen from the figure, the microcrystalline material before adsorption shows a loose and irregular rod-like structure, and the microcrystalline material after adsorption of fluorocarbon has a smooth and compact columnar structure with uniform distribution and smaller

pores, which conforms to the adsorption characteristics of the adsorbent.

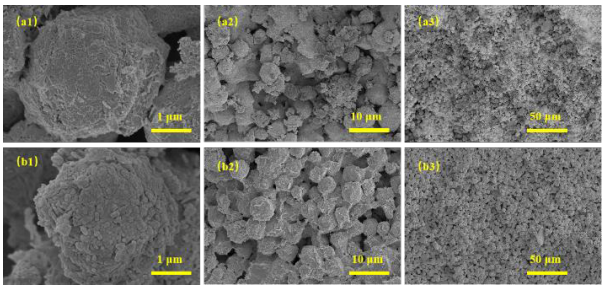

Fig. 2 SEM images of microcrystalline materials before and after adsorption of fluorocarbon: (a) before adsorption; (b) After adsorption.

3.2 The optimal processing temperature for thermogravimetric analysis.

In thermal analysis, the reaction rate of microcrystalline materials varies with temperature, which is obtained by observing the change of its mass and the decomposition rate varying with temperature when heating the sample at a fixed heating rate[10]. According to the thermal analysis kinetics theory, the pyrolysis process of microcrystalline material adsorbent is generally expressed as[11]:

$$A(s) \rightarrow B(s) + C(g) \tag{1}$$

In heterogeneous systems and non-isothermal conditions, the reaction kinetics equation is expressed as[12]:

$$\frac{d\alpha}{dT} = \left(\frac{1}{\beta}\right) k(T) f(\alpha) \tag{2}$$

Where: T is the thermodynamic temperature, K; β is the heating rate (generally constant), ℃/min; α is the conversion rate, generally, $\alpha = \frac{W_0 - W}{W_0 - W_\infty}$, W_0 is the original mass of the adsorbent, W is the residual mass of the adsorbent at the temperature of T, and W_f is the residual mass of the adsorbent at the end of pyrolysis; $f(\alpha)$ is the expression of reaction mechanism.

The relationship between $k(T)$ and thermodynamic temperature T can be expressed by Arrhenius equation[13]:

$$k = A\exp\left(-\frac{E}{RT}\right) \tag{3}$$

Where: A stands for pre-exponential factor; E represents apparent activation energy; R represents the molar gas constant, 8.314 J/(mol•K).

The equation obtained by simultaneous expression (2) and expression (3) is:

$$\frac{d\alpha}{dT} = \frac{A}{\beta}\exp\left(-\frac{E}{RT}\right) f(\alpha) \tag{4}$$

After performing differentiation and integration on equation (4), the parameters can be determined. The differential method calculates the first derivative of temperature by using the conversion rate. The process of integration necessitates the introduction of a temperature incorporation formula to integrate equation (4) on both sides. Nonetheless, the integral form frequently leads to imprecise outcomes, hence an estimated formula is commonly employed in lieu of the integration formula to facilitate computation[14, 15].

3.2.1 Pyrolysis Characteristics of Microcrystalline Materials

Temperature is one of the important factors affecting the desorption performance of adsorbents. Thermogravimetric analyzer was used to heat the adsorbed microcrystalline material to 900℃ at four different heating rates of 5, 10, 20 and 30 ℃/min. As shown in Figure 3, the weight loss rate of microcrystalline material adsorbent is about 20% between room temperature and 300℃, which is a rapid pyrolysis stage. After the temperature reaches 300℃, the TG curve is gradually flat, which shows that the gas adsorbed in microcrystalline materials has basically been desorbed in the rapid pyrolysis stage, and the desorption effect is not obvious if the temperature continues to increase. Therefore, it can be preliminarily determined that the optimal treatment temperature of CF-100 microcrystalline material adsorbent is 300℃.

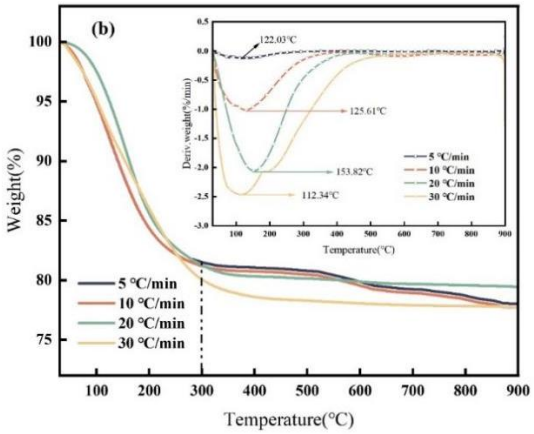

Fig. 3 TG/DTG curves of microcrystalline materials before and after adsorption at different heating rates.

3.2.2 Solution of thermodynamic parameters

Based on the recommendations of the ICTAC kinetics committee, due to the complex nature of the carbon fluorine adsorbent material in this experiment, a non-model method was employed to directly obtain kinetic parameters for different conversion rates. This approach avoids the limitations of conducting thermokinetic research using a single TG curve and reduces errors caused by differences in thermokinetic mechanisms.

In this study, the Flynn-Wall-Ozawa (FWO) integral method was selected for the calculation of activation energy, and the corresponding equation is shown below[16]:

$$\lg\beta = \lg\left(\frac{A_F E_F}{RG(\alpha)}\right) - 2.315 - 0.4567\frac{E_F}{RT} \quad (5)$$

Where E_F is the average activation energy calculated by FWO method, KJ/mol. Through the utilization of Equation (5), with varying conversion rates and four distinct heating rates, and the corresponding thermodynamic temperatures, a determination of activation energy was made by analyzing the slope of the curve produced by the lgβ-1/T relationship. The resulting calculation for E_F yielded a value of 293.933 KJ/mol. The high linearity of the fitting degree at different conversion rates in Figure 4 illustrates the accuracy of the FWO method in analyzing the pyrolysis process results. This method avoids the use of reaction mechanism functions and directly calculates the activation energy. The range of α is selected as 0.05 to 0.7, and linear fitting is performed under different heating rates of 5, 10, 20, and 30 ℃/min. The data presented in the diagram reveals that when the value of α exceeds or equals 0.4, there is observed variance in the activation energy with respect to α. This phenomenon is indicative of a shift in the decomposition mechanism of the sample, which raises the possibility of the presence of a multi-stage decomposition mechanism having multiple types of bonds and a multitude of phase conversion characteristics.

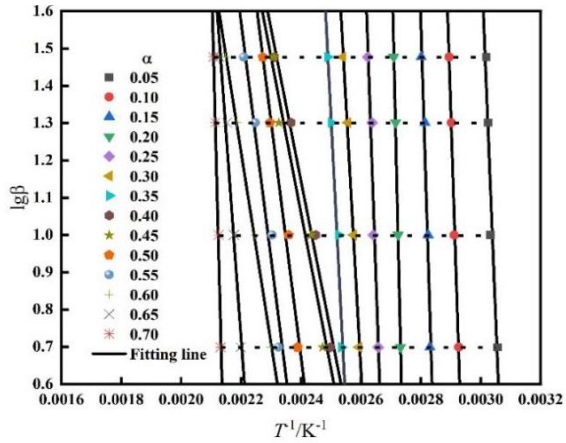

Fig. 4 Relationship between apparent activation energy and different conversion rates

3.3 Optimal processing time for infrared analysis

The adsorption capacity measurements for Group B microcrystalline materials with varying processing durations are illustrated in Figure 5(a). When the treatment duration is below 2 h, the specific surface area and specific volume both elevate as the heat treatment time increases. They culminate at 2 h, implying that the optimal restoration of the adsorption capacity in microcrystalline materials is achieved after 2 h of heat treatment.

Subsequently, Fourier transform infrared spectrometer (FTIR) was used to analyze the chemical composition of group B microcrystalline materials with heat treatment time of 0 h and 2 h, respectively. As shown in Figure 5(b), there were strong absorption peaks at wave numbers of 979.27 and 949.39 cm^{-1}, which were the main characteristic peaks of fluorocarbon, and the wave number peaks of microcrystalline materials with treatment time of 0 h were higher than those of 2 h, indicating that the longer the treatment time, the decrease or even disappearance of C_3F_8 and C_2F_6.

Absorption peaks are observed at wavenumbers around 3475, 1640, and 660 cm^{-1}, which are attributed to the asymmetric stretching and bending vibrations of the O-H bond in water molecules. The microcrystalline material treated for 2 h shows a significant decrease in water content. Absorption peaks between 440 and 754 cm^{-1} are decomposition products of SF_6, such as SOF_4 and SO_2F_2. With the prolongation of processing time, the absorption peaks of characteristic products weaken until they disappear. This indicates that under the conditions of a thermal treatment temperature of 300℃ and a time of 2 h, the desorbed gas inside the adsorbent can be significantly reduced.

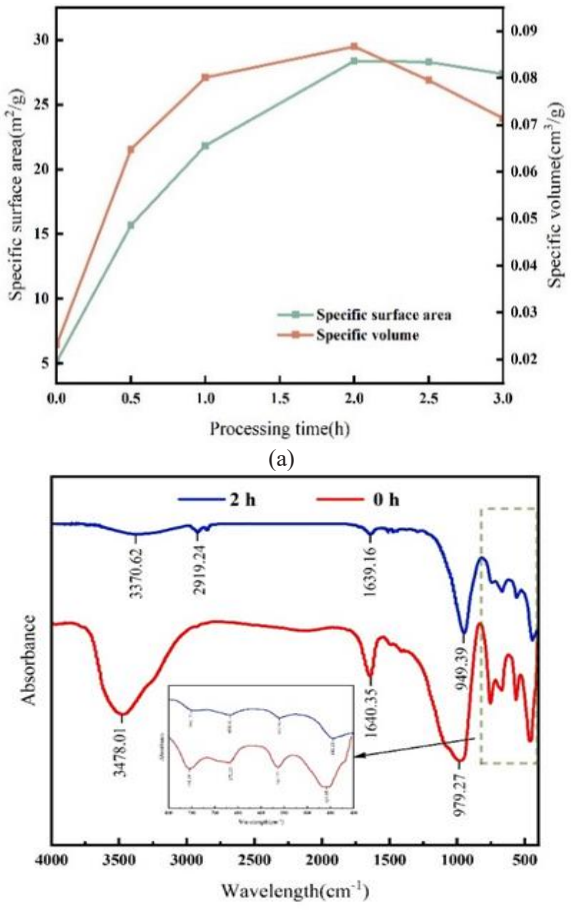

Fig. 5 Adsorption capacity index and infrared spectrum of group B microcrystalline materials at different treatment times

3.4 Test results of regeneration performance of microcrystalline materials

3.4.1 Cycle stability evaluation of different regeneration methods

The cycling stability of adsorbents is one of the important factors for evaluating the regeneration performance, and

it is closely related to the regeneration method of the adsorbent. Therefore, two regeneration methods, vacuum desorption with vacuum pumping and vacuum desorption with auxiliary heating, mentioned in the previous text, were selected to evaluate the cycling stability of the microcrystalline material.

Saturated adsorption capacity refers to the adsorption capacity of fluorocarbon under the equilibrium pressure of 1.0 MPa. The relationship between the regeneration capacity of CF-100 microcrystalline material adsorbent and the regeneration times is shown in Figure 6. From the figure, it can be seen that with the increase of the regeneration times, the adsorption capacity of fluorocarbon changes after two regeneration methods, in which the adsorption capacity of fluorocarbon of microcrystalline material decreases slightly after five times of vacuum pumping and high temperature regeneration, and it is almost ignored, while the adsorption capacity of fluorocarbon decreases greatly after the third vacuum pumping regeneration. The experimental device can realize two kinds of desorption and regeneration experimental functions well. The experiment proves that the desorption and regeneration mode of microcrystalline material adsorbent for fluorocarbon in SF_6 is better than vacuum regeneration. Therefore, the vacuum desorption regeneration performance of auxiliary heating is explored later.

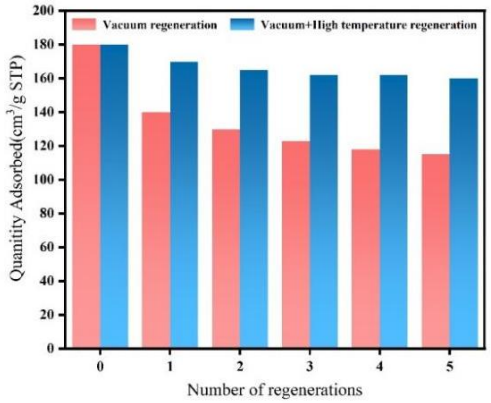

Fig. 6 Relationship between regeneration ability and regeneration times of CF-100 microcrystalline material adsorbent

3.4.2 Study on regeneration performance of high temperature desorption

The adsorption isotherm is a curve depicting the variations in adsorption quantity or adsorption rate of an adsorbent with respect to changes in pressure under constant temperature conditions[17]. It is an essential tool for evaluating the separation process between adsorbates and adsorbents. IUPAC classifies the latest adsorption isotherms into six types, namely, type I Langmuir isotherm, type II S isotherm, type III isotherm (without B inflection point) (the adsorption force between sample and adsorbate is smaller than that between adsorbate), type IV isotherm (with hysteresis loop) (the curve at the beginning of the curve bulges upward, and the isotherm at the end of the curve rises sharply due to capillary condensation), and type V isotherm (with a higher bulge toward the opposite pressure axis), VI type step isotherm[18]. Since the fluorocarbon in SF_6 gas in high-voltage electrical equipment is a mixed gas containing C_2F_6 and C_3F_8, the adsorption isotherm curve equation of the mixed gas, that is, the extended Langmuir equation[19], can be derived by the principle of adsorption potential energy and adsorption heat.

$$q_i = \frac{q_{mi} B_i p_i}{1 + \sum_{j=1}^{n} B_j p_j} \tag{6}$$

In the equation, q represents adsorption amount; q_m represents the saturated adsorption amount; p represents total pressure; B represents Langmuir constant. When correlating data, the Langmuir linear form is commonly used:

$$\frac{1}{q} = \frac{1}{q_m} + \frac{1}{q_m B p} \tag{7}$$

The adsorption parameters B and q_m of single gas can be obtained by using the relationship curve of $\frac{1}{q}$ to $\frac{1}{p}$, and then the adsorption amount of mixed gas can be further predicted by formula (6). At the same time, the specific surface area S_g and specific volume V_m of the adsorbent can be obtained respectively according to the measured adsorption parameters q_m of mixed gas combined with formula (8) and formula (9):

$$S_g = q_m \cdot A \cdot \sigma_m \tag{8}$$

$$V_m = \frac{q_m \times 44}{22400 \rho_m} \tag{9}$$

Where: A represents Avon Gadereau constant, which is 6.02×10^{23}; σ_m is the cross-sectional area of adsorbate molecules; ρ_m is the density of adsorbed phase molecules at 273 K.

The specific surface area and pore size of microcrystalline materials undergo variations with changes in their adsorption capacity. By examining the adsorption data of three groups of microcrystalline materials, namely A, B, and C, with varying adsorption capacities before adsorption, after reaching saturation, and after a 2-hour desorption process, the ability of the microcrystalline material to regenerate after high temperature desorption can be assessed. Figure 7 shows the adsorption-desorption isotherms and pore size distribution charts of three groups of microcrystalline materials A, B, and C. The curves exhibit type IV isotherms and H3 hysteresis loops, indicating that these materials possess mesoporous structures. They undergo monolayer adsorption before proceeding to multilayer adsorption.

The specific surface area and pore structure of groups A, B and C microcrystalline materials are shown in Table 3. From the experimental results in the table, it can be seen that the specific surface area and pore volume of CF-100 microcrystalline materials decreased from 31.669 m^2/g and 0.1074 cm^3/g to 5.1280 m^2/g and 0.0231 cm^3/g,

respectively, and the pore size increased from 12.111 nm to 17.525 nm. It shows that the adsorbent has reached the threshold of adsorption capacity, the number of adsorption molecules is low, and the adsorption capacity has reached a great loss. After desorption at 300℃ for 2 h, the specific surface area rebounded rapidly, and the specific surface area was slightly lower than that without adsorption, which indicated that the regeneration recovery performance was high.

Table 3 List of specific surface area and pore structure of three groups of microcrystalline materials A, B and C.

Parameters	Samples		
	Non-adsorption	After adsorption	Desorption 2 h
S_{BET}(m^2/g)	31.669	5.1280	28.365
V_{mes}(cm^3/g)	0.1074	0.0231	0.0867
D_{ave}(nm)	12.111	17.525	13.163

S_{BET}: specific surface area measured by the BET method, V_{mes}: mesopores pore volume, D_{ave}: average pore diameter

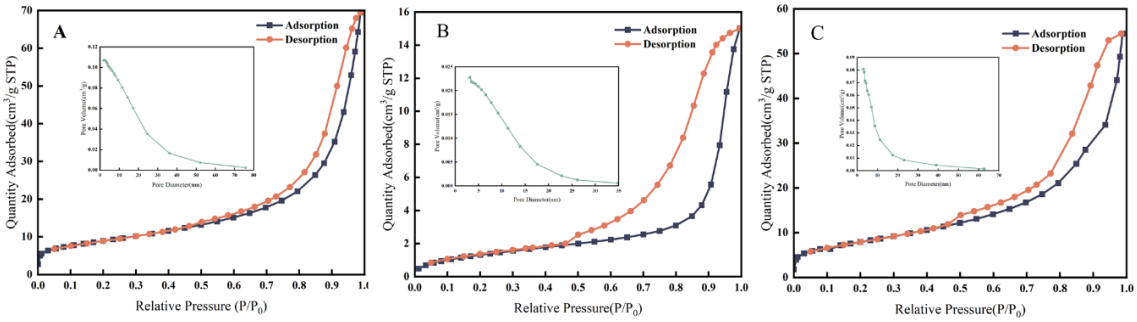

Fig. 7 A, B and C adsorption-desorption isotherms and pore size distribution diagrams of three groups of microcrystalline materials.

4 Conclusion

Based on the experimental device of fluorocarbon adsorbent desorption, which can simultaneously realize Vacuum desorption of auxiliary heating and vacuum desorption, The relationship between adsorption performance and regeneration times, thermogravimetric analysis, infrared spectrum and other characterization methods were used to compare the regeneration performance of CF-100 microcrystalline materials with two regeneration technologies. Get the following conclusions:

(1) Before adsorption, the microcrystalline material had a loose and irregular rod-like structure. After adsorption, the microcrystalline material exhibited a smooth and more compact cylindrical structure that was evenly distributed, with smaller pores, which is in line with the adsorption characteristics of adsorbents.

(2) Analyze the relationship between regeneration ability and regeneration times of CF-100 microcrystalline material adsorbent: The stability of two regeneration methods for desorption is excellent. After five times of vacuumizing and high temperature regeneration, the adsorption capacity of fluorocarbon in microcrystalline materials decreased slightly. However, the adsorption capacity of carbon fluoride decreased greatly after the third vacuum regeneration. It demonstrates that the desorption and regeneration method of carbon fluorides in SF_6 by using microcrystalline material adsorbents shows that the stability of vacuum desorption and regeneration cycle with auxiliary heating is better than that of vacuum regeneration.

(3) According to the data of thermogravimetry and Fourier infrared spectrum, it is concluded that the high temperature desorption reaches the optimal desorption condition when heating treatment is carried out at 300℃ for 2 h, Through the relationship between apparent activation energy and different conversion rates, it is known that when $\alpha \geq 0.4$, the activation energy fluctuates with the change of α, and the decomposition mechanism of the sample changes, indicating that there is a multi-stage decomposition mechanism with the diversity of bonds and the multiphase characteristics of their conversion, and the activation energy is 293.933 KJ/mol.

(4) By examining the adsorption data of three groups of microcrystalline materials, with varying adsorption capacities before adsorption, after reaching saturation, and after a 2-hour desorption process, it is concluded that the specific surface area of microcrystalline materials decreases from 31.669 m^2/g to 5.1280 m^2/g after adsorption of fluorocarbon. It shows that the adsorption threshold has been reached at this time, the number of adsorbed molecules is low, and the adsorption capacity has reached a great loss. After desorption at 300℃ for 2 h, the specific surface area increased to 28.365 m^2/g, indicating that the regeneration recovery performance was high.

Acknowledgments

This paper is a general project of the National Social Science Fund "Science and Technology Project of State Grid Anhui Electric Power Co., Ltd." (52120522000L)

References

1. Xiao, S., Shi, S.Y., Lin, J.T. (2023) Analysis on the Control Strategy of the Strong Greenhouse Insulating Gas SF6 in High-voltage Electrical Equipment Under the Goal of “Emission Peak and Carbon Neutrality”. Proceedings of the CSEE., 43(01):339-358.
2. Luo, Q. (2022) Xi Jinping’s Important Statements on Peak Carbon Dioxide Emissions and Carbon Neutrality：Logical Thought，Value Implication and Practice Path. Governance Modernization Studies., 38(04):5-13.
3. GB/T 12022-2004 National Standard for Industrial Sulfur Hexafluoride.
4. Ji, Y.S., Zhang, M., Wang, C.Y., et al. (2021) Study on Decomposition Products of SF6/N2 Gas Mixture Under

the Action of Electric Arc. High Voltage Apparatus., 57(03):145-151+156.

5. Peng, W.W., Shen, X.L., Qian, Y.Q., et al. (2023) Research on Recognition and Diagnosis of Latent Faults of GIS Equipment. NORTHEAST ELECTRIC POWER TECHNOLOGY., 44(08):51-55.
6. Ye, Q.B. (2022) Integrated Technology of Deep Desulfurization and Naphthalene Removal of Coke Oven Gas Based on Microcrystalline Adsorption Process. Shaxi Metallurgy., 45(05):69-70+90.
7. Lu, H., Li, B.X., Sun, B.P., et al. (2023) Crystal Growth and Laser Performance Research Based on Nd: LiLuF4 Microcrystalline Materials. JOURNAL OF SYNTHETIC CRYSTALS., 52(07):1250-1257.
8. Chen, S.H., Liu, X.W., Zou, J.P., et al. (2017) Experimental Study of the Adsorption of CH4/CO2 Mixture by the Regeneration of Molecuar Sieve. The Journal of New industrialization., 7(11):68-72.
9. Chen, P. (2022) INEOS Polypropylene Plant Start-up and Shutdown Process Safety Risks and Solutions. Chemical Enterprise Management., (28):111-114.
10. Chen, Y.X., Zhou, D.S., Hu, W.B. (2021) Progress of Differential Scanning Calorimetry and Its Application in Polymer Characterization. ACTA POLYMERICA SINICA., 52(04):423-444.
11. Vyazovkin, S., Burnham, A.K., Criado, J.M., et al. (2021) ICTAC Kinetics Committee recommendations for performing kinetic computations on thermal analysis data. Thermochimica Acta., 520(1-2):1-19.
12. Huang, Z., Feng, B.B., Zhang, X.R., et al. (2014) Introduction of Thermal Decomposition Kinetic Analysis and Calculation Models. CHINA PRINTING AND PACKAGING STUDY., 6(06):4-17.
13. Minkoo, K., Sunjae, L., Ho, J.K., et al. (2022) Remaining useful life estimation using accelerated degradation test, a gamma process, and the arrhenius model for nuclear power plants. Journal of Mechanical Science and Technology., 36(10):4905-4912.
14. Liu, X.F., Yang, P.B., Wang, J., et al. (2021) Co-Pyrolysis Characterisistics and Kinetic Analysis of Wheat Straw and Lignite. ACTA ENERGIAE SOLARIS SINICA., 42(09):410-415.
15. Zhang, D.R., Lu, L.G. (2021) Pyrolysis and Thermokinetic Characteristics of Calixarene. CHINA PLASTICS., 35(11):104-110.
16. Jiang, G.D., Wei, L.P., Teng, H.P., et al. (2017) A kinetic model based on TGA data for pyrolysis of Zhundong coal. CIESC Journal., 68(04):1415-1422.
17. He, X.D., Zhu, M., Chen, G.Q., et al. (2021) Study on Isotherm Distridution of Low Temperature and Low Pressure Adsorption of Low Temperature Adsorbent. China Special Equipment Safety., 37(04):18-23+74.
18. Cheng, Y.T., Li, B.Y., Li, Z. (2023) MOFs-Based Carbon Materials for Adsorption and Removal of Antibiotics in Water Body. Water Purification Technology., 42(04):31-38.
19. Wei, G., Wang, J.G., Xia, Y.Y., et al. (2014) Regeneration technology of SF6 -molecular-sieve adsorbent using vacuum heat treatment. CHEMICAL ENGINEE R ING(CHINA)., 42(11):35-3.